9th ASM CONFERENCE ON

ADVANCES IN THE PRODUCTION OF TUBES, BARS AND SHAPES

9th ASM CONFERENCE ON

ADVANCES IN THE PRODUCTION OF TUBES, BARS AND SHAPES

Sponsored by the ASM Extrusion and Drawing Committee of the
MECHANICAL WORKING AND FORMING DIVISION

22-24 April 1985
Cincinnati, Ohio

Library of Congress Catalog Card Number: 85-072289

ISBN: 0-87170-213-4

SAN: 204-7586

Printed in the United States of America

CONFERENCE ORGANIZING COMMITTEE

Charles S. Cook, Chairman
Westinghouse Research & Development
Pittsburgh, Pennsylvania

John Walters, Vice Chairman
Cameron Iron Works Inc.
Houston, Texas

Michael E. Celovsky
Industrial Tool Engineering Co.
Detroit, Michigan

Fred Cole
AMAX Specialty Metals Corp.
Coldwater, Michigan

Frank J. Cornwell
Uniform Tubes, Inc.
Collegeville, Pennsylvania

Walt Drabold, Jr.
Morgan Construction Company
Stow, Ohio

James C. England
Huntington Alloys, Inc.
Huntington, West Virginia

Robert J. Fiorentino
Battelle-Columbus Laboratories
Columbus, Ohio

Jim Henderson
RMI Company
Ashtabula, Ohio

Willie A. Houle
Noranda Metal Industries Ltd.
Montreal, Quebec, Canada

William G. Janis
Century Specialties
Traverse City, Michigan

Mac McClanahan
Teledyne Wah Chang
Albany, Oregon

Geoffery Tetley
McQuay Perfex, Inc.
Grenada, Mississippi

Ike Tripp, Sr.
Etna Products
Chagrin Falls, Ohio

PREFACE

The well known changes in energy cost and availability and changes in competition from a national to international basis have produced changes in all aspects of manufacturing toward the necessity for simultaneous improvements in both manufacturing efficiency and product quality. In order to achieve these objectives it is necessary to develop and apply the most advanced technologies in metallurgy and metals processing. In response to this need, the ASM Extrusion and Drawing Committee sponsors conferences on 18 month cycles which are entitled "Advances in the Production of Tubes, Bars, and Shapes" which provide a forum for presentation and discussion of advanced metalworking technologies. These Proceedings of the most recent, Ninth Conference on April 22-24, 1985, include papers on the direct conversion of powder to rod and wire, multi-alloy tubular products through powder metallurgy, the theoretical experimental analyses of extrusion and mandrel mill processes, and the integration and control of sequences of production procedures using computers and statistical analyses. Taken together these papers represent the state-of-the-art and an indication of the future direction for development. We hope you find these proceedings of value and look forward to your comments, suggestions, and future participation.

Charles S. Cook

Foreword

The Ninth Conference on the Advances in the Production of Tubes, Bars, and Shapes was held on April 22-24, 1985, in Cincinnati, Ohio. The Conference was sponsored and organized by the Extrusion and Drawing Committee of the American Society for Metals, Metalworking and Forming Division. In addition to the authors, the Conference participants were Mr. Charles Cook, Westinghouse Electric Corporation, Conference General Chairman and Committee Chairman and session chairs: Mr. John Walters, Cameron Iron Works, Inc.; Mr. Walt Drabold, Morgan Construction Company; Mr. Jim Henderson, RMI Company; and Mr. Fred Cole, AMAX Specialty Metals Corporation. Administrative assistance in the organization of the conference and in the publication of these proceedings was provided by Ms. Shari Gerstenberger, Mr. Bob Uhl, Mr. Don Varansese, and Ms. Joan Bellian of the American Society for Metals.

Charles S. Cook
Chairman

TABLE OF CONTENTS

SESSION I

SESSION II

SESSION III

SESSION IV

STRAIN FIELDS FOR ALUMINUM AT DIFFERENT TOOLING TEMPERATURES AND EXTRUSION RATIOS

H.B. Peacock
Savannah River Laboratory
Aiken, SC, USA

D.G. Berghaus
Georgia Institute of Technology
Atlanta, GA, USA

ABSTRACT

STRAIN DISTRIBUTIONS throughout the die region are obtained for axisymmetric extrusion of aluminum billets. Results which include the three extensional strains and accumulated shear are produced from an analysis of experimentally obtained laminar flowlines on extruded specimens. Extrusion experiments are performed at average tooling temperatures of 175°C and 354°C and for extrusion ratios from 1.9 to 12.4. Both tooling temperatures and extrusion ratios affect the magnitude and/or the distribution of plastic strains in extruded aluminum.

LARGE PLASTIC STRAINS are produced when an aluminum billet is extruded through a conical die. These strains are related to the formation of extrusion defects. The finite strain distribution cannot be calculated theoretically but can be determined experimentally. Originally, Thomsen, Yang, and Kobayashi[1] proposed an experimental method, commonly referred to as visioplasticity, to evaluate plastic deformation in metalworking processes. The analysis is based on determining velocity components from flowline profiles.

In this paper, visioplasticity is used to find the magnitude and distribution of strains for axisymmetric extrusion of solid aluminum billets. Strain development is evaluated as a function of extrusion tooling temperature and extrusion ratio (R).

VISIOPLASTICITY ANALYSIS

Visioplasticity is a technique employed to evaluate strain and strain rate fields during plastic deformation. The technique is based upon observations of changes in line patterns applied to a work piece prior to any metal working operation. Medrano and Gillis[2] presented a visioplastic method for axisymmetric extrusion. Their technique was adapted for this study. Improved numerical methods for strain calculations were incorporated into a computer program at the Savannah River Laboratory for the strain analysis of partially extruded solid aluminum billets.[3]

A rectangular grid is placed on the central plane of the billet in allignment with the billet axis. After partial extrusion, lines initially parallel with the billet axis are deformed so that they indicate the material flow path through the die region. These are called flowlines. Lines initially normal to the billet axis are deformed to indicate the extent of metal flow. These are called isochronal lines.

Visioplastic strain analysis is based on the flow path described by the flowlines. An axisymmetric flow function ϕ is defined such that

$$\phi(r) = 2\pi \int_0^r \zeta v \, d\zeta \qquad (1)$$

where r is the radial distance to a given flowline and v is the velocity in the axial direction. The flow function is equivalent to the volume flowrate through a circular area of radius r from the axis to the flowline.

The axial and radial velocities for the material are written in terms of the flow function and the billet radius because all flow takes place along flowlines and because ϕ is constant along a given flowline. There is no material transfer across flowlines.

The strain rates in polarcylindrical coordinates are determined as derivatives of the velocity components. These rates are transformed into curvilinear coordinates and integrated using kinematic relationships for spatial integration. The equation for strains in the axial direction (z) along each flowline is

$$\varepsilon_i(z), \gamma_{ij}(z) = \int_{z_o}^{z} \frac{\dot{\varepsilon}_i(z), \dot{\gamma}_{ij}(z)}{v} \, dz \qquad (2)$$

Integrated extensional strain values are defined as ε_a along the flowline, ε_b perpendicular to the flowline, and ε_θ circumferential with respect to the flowline. The integrated shear strain rates are referred to as "accumulated shear," γ_{ab}, because the classical definition of shear strain limits the value to $\pi/2$.

EXPERIMENTAL PROCEDURE

Billets were made from commercial Alcoa 1100 aluminum. Solid cylindrical stock was split along the axis into equal half sections and the surfaces were milled flat. The two sections were then reasssembled and machined to 8.9 cm (3.5 in.) in diameter and 10.2 cm (4.0 in.) long.

A retangular grid was ink stamped onto the axial plane of one of the two billet halves. High temperature black industrial marking ink (No. 550, Phillips Process Co., Inc., Rochester, N.Y.) was used to stamp the grid because all tests were done at billet temperatures of approximately 425°C. The grid consisted of 1.27 mm (0.05 in.) squares. Alignment of the grid was accomplished using a specially designed fixture to hold the half billet and the stamp.

After the ink dried, the billet halves were assembled and tack welded on both ends by gas-tungsten-arc welding (GTA). The assembly was placed into a snug fitting aluminum canister of 0.64 mm (0.025 in.) wall thickness. The canister was heated to 200°C and the outside surface was coated with a graphite-clay lubricant.

Extrusion was performed on a 4.4×10^6N (500-ton) laboratory extrusion press with a ram speed of 45.7 cm (18 in.) per minute. Conical converging dies with a 45 degree semicone angle were used in all extrusion tests. The extrusion container and die were heated with electrical resistance heaters and the billet was preheated in an electrical resistance furnace. The extrusion tooling and the outside surface of the billet were lubricated again before extrusion with a mixture of lead powder and oil in a ratio of one to three by volume. The billet was partially extruded to about half the original length. The extrusion press was stopped and the extruded rod was sawed off approximately three inches from the die exit. The partially extruded billet was then removed from the container and broken open to show the deformed grid.

The grid pattern was photographed and enlarged to about three and a half times the original size. Flowlines were placed into discrete digital form using a Data Tablet Digitizer model HW-11/48 (Summagraphics, Fairfield, Connecticut). The tablet contained 78.7 lines per cm (200 lines/in.) giving a resolution of 0.1 mm (0.005 in.).

Effects on the magnitude and distribution of strains were evaluated for different tooling temperatures and extrusion ratios. The tooling temperature ($\bar{T}$) for a given extrusion condition was determined as an arithmetic average of the temperatures of the container and die. The low tooling temperature was 175 $\pm$ 1°C while the high tooling temperature was 354 $\pm$ 10°C. Extrusion ratios ranged from 1.9 to 12.4. Extrusion parameters for each test are given in Table 1.

RESULTS AND DISCUSSION

The following results are presented for extensional strains ε_a, ε_b, and ε_θ and accumulated shear γ_{ab}. The effect of tooling temperature and extrusion ratio on the strain magnitude and distribution were determined by using, as nearly as possible, identical extrusion parameters. The extrusion ratio was constant when investigating tooling temperature effects while the average tooling temperature was constant when investigating extrusion ratio effects. The extrusion ratio was calculated by the area method.

TOOLING TEMPERATURE - The magnitude and distribution for the three extensional strains ε_a, ε_b, and ε_θ are shown in Figures 1, 2, and 3 for both low and high tooling temperatures. The extrusion ratio is 12.4. Strain contour lines are shown on billet half cross-sections for strain increments of 0.25. Each contour line represents constant extensional strain or constant accumulated shear values. Contours for the three different extensional strains appear similar at the low and the high tooling temperatures. Thus, extensional strains seem largely independent of the tooling temperature. The magnitude of the three extensional strains increases systematically as the material moves through the tapered region toward the die exit. The largest strain contours shown on the figures are +2.5 for ε_a, parallel to the flowlines, -1.25 and -1.5 for ε_b perpendicular to the flowlines, and -1.25 for ε_θ circumferential to the flowlines. Strain contour lines for ε_a and ε_θ indicate that a relatively smooth strain distribution exists in the deformed material. However, the strain contour lines for ε_b are shifted toward the die exit in a narrow region parallel and close to the billet surface. This displacement of the contour lines indicates a region of lower strain in the material.

The accumulated shear contour lines are shown in Figure 4 for both low and high tooling temperatures at an extrusion ratio of 12.4. The magnitude and distribution of the accumulated shear are changed significantly in the deformed region at the different tooling temperatures. The maximum accumulated shear contour line on the figure for the low tooling temperature is much larger than for the high tooling temperature. The largest accumulated shear values are in the upper part of the material near the surface of the rod.

In Figure 5 are shown the final extensional strains and final accumulated shear values in the extruded rods for both low and high tooling temperatures. The extrusion ratio is 12.4. Strains are plotted as a function of the radius of the rod. Extensional strain values for ε_a and ε_b are almost constant along the radius except near the surface of the rod where the

strain magnitudes increase. The individual values for ε_θ are practically constant across the entire rod radius. The difference between individual extensional strains at low and high tooling temperatures is less than 5%. Extensional strains, as pointed out from strain contour plots, are considered essentially independent of the tooling temperature.

Large differences occur in the magnitude and distribution of the accumulated shear γ_{ab} for low and high tooling temperatures. At low temperature, the shear distribution along the radius has peak positive and negative values while at high tooling temperature, the distribution oscillates with mostly negative shear. The largest accumulated shear values occur near the edges. For low tooling temperature, the maximum shear is -3.0 and for high tooling temperature, the maximum shear is -1.5. The peak accumulated shear value at high tooling temperature is half the maximum value at low tooling temperature and is found closer to the surface of the extruded rod.

EXTRUSION RATIO - Extensional strain contour lines for 1.9, 7.4, and 12.4 extrusion ratios are shown in Figures 6, 7, and 8. The tooling temperature is 354°C. At an extrusion ratio of 1.9, compressive ε_a strains, down to -0.25, appear in the upper part of the deformed region while relatively smooth tensile strain contours, up to +0.50, form near the die exit. As the extrusion ratio increases, extensional strains parallel to the flowlines become tensile in the conical part of the die and increase to a maximum value at the die exit. For ε_b, a region of tensile strain occurs at the die entrance for an extrusion ratio of 1.9 while compressive strains exist elsewhere in the material. An increase in the extrusion ratio increases the compressive strain normal to the flowlines at the die exit. The displaced part of the contour lines, located near the edge and parallel to the die surface, is more pronounced for the 12.4 extrusion ratio. Contour lines for ε_θ are relatively uniform. As the extrusion ratio increases, values for the extensional strains ε_a, ε_b, and ε_θ at the die exit increase so that the magnitudes are a function of the extrusion ratio.

The accumulated shear (γ_{ab}) contour lines are shown in Figure 9 for different extrusion ratios. At an extrusion ratio of 1.9, compressive shear contours with magnitudes down to -0.25 extend back into an area near the die wall preceding the tapered region of the die. Large shear values up to -1.0 occur close to the die wall. For extrusion ratios greater than 1.9, the accumulated shear contour lines are primarily inside the tapered region and show relatively steep gradients near the outside surface of the material.

Final extensional strains and accumulated shear values in extruded rods are shown in Figure 10 for the three different extrusion ratios. The data are plotted as a function of the rod radius. Also shown are values for logarithmic strains calculated at the die exit. Extensional strains ε_a, ε_b, and ε_θ are functions of the extrusion ratio as indicated by the contour plots, and increase in magnitude as the extrusion ratio increases. The value for the circumferential strain ε_θ is practically constant across the rod cross section while the absolute values for ε_a and ε_b tend to increase, especially near the edges as previously noted.

The magnitudes for the average circumferential logarithmic strains agree well with experimentally determined ε_θ values. Although logarithmic values are close for ε_a and ε_b, calculations using logarithmic geometrical relationships are not theoretically valid due to shearing action in the extruded material.[3]

The accumulated shear curves for 1.9 and 7.4 extrusion ratios exhibit somewhat sinusoidal shapes. At an extrusion ratio of 12.4, the accumulated shear curve shows multicycles, as mentioned earlier, with mostly negative shear. Two peak values occur in the distributions, one near the surface and the other approximately midway along the radius. The largest shear values are found near the edge of the rod and range from -1.15 to -1.5 for the three different extrusion ratios..

ACCURACY - Two tests may be performed to evaluate the accuracy of the experimental and numerical procedures. The first test consists of a numerical intergration of the velocity to find the elapsed time value for each solution station. Values obtained are then interpolated to determined constant time contours for comparison with the experimental isochronal curves. The isochronal curves are not used in the solution for the strains.

Such tests of isochronals are carried out for specific points for each of the extrusions. The comparisons are given in Figure 11 for 1.9 and 12.4 extrusion ratios at the high tooling temperature. While the comparisons are generally good, there is a tendency for separation between the experimental curves and numerical values near the die wall particularly at low extrusion ratio. This has been experienced in other analyses.[3,4]

A second test can be applied by comparing circumferential strains along the radius at the die exit with logarithmic geometric values for large strain. Results will be compared for the circumferential strains although values for strains parallel and normal to the flow lines are equally good. For a given flowline which has an initial radius of R_i before the die entrance, and a final radius of R_f after extrusion, the logarithmic circumferential strain may be written:

$$\varepsilon_{\theta l} = \ln\left(\frac{2\pi R_f}{2\pi R_i}\right) = \ln\frac{R_f}{R_i} \qquad (3)$$

The comparison of ε_θ with $\varepsilon_{\theta l}$ along the radius is good everywhere at the die exit except very near the billet axis. Here, the value of the logarithmic circumferential strain is sometimes

slightly larger due to the small radii of the numerically approximated flowlines. The circumferential logarithmic strains are very close to the calculated average circumferential strains at the exit. Calculations for average strains are based on the volume of material experiencing strain. The largest difference between calculated and experimental values occurs for the 1.9 extrusion ratio and is less than 10%. Comparisons for the circumferential strains are shown in Table II.

The plastic zone size determined from the strain contour lines is basically confined within the tapered region of the die. The shape is similar to the plastic zone configuration formulated by Lambert and Kobayashi[5] for extrusion through conical dies with low interface friction.

SUMMARY AND CONCLUSIONS

Large plastic strains often cause extrusion defects. Extrusion parameters that reduce the strain magnitude or alter the distribution may decrease the tendency for defect formation. The effect of tooling temperature and extrusion ratio on the magnitude and distribution of large plastic strains in solid aluminum billets was determined using visioplasticity. The conclusions were that:

1. The magnitude and distribution of the three extensional strains for aluminum are practically independent of the extrusion tooling temperature. On the other hand, the accumulated shear is a function of tooling temperature with high temperature giving much lower shear values and altering the radial distribution. Maximum accumulated shear occurs closer to the surface of the rod extruded at high tooling temperature.
2. Extensional strains in aluminum are increasing functions of the extrusion ratio. Average extensional strains at the die exit agree well with calculated values determined using logarithmic geometrical relationships for large strain. The maximum accumulated shear can not be calculated theroetically but can be determined experimentally. The maximum accumulated shear value at high tooling temperature increases 30% when the extrusion ratio goes from 1.9 to 7.4 but remains about the same value between 7.4 and 12.4. The distribution for the accumulated shear changes with the extrusion ratio. Two peak values occur, one near the surface and the other approximately midway along the radius.

ACKNOWLEDGEMENT

The information contained in this article was developed during the course of work under Contract No. DE-AC09-76SR00001 with the U.S. Department of Energy.

REFERENCES

1. Thomsen, E. G., C. T. Yang and S. Kobayashi, "Mechanics of Plastic Deformation in Metalworking," pp. 166-167, MacMillan, New York (1965).

2. Medrano, R. E. and P. P. Gillis, Journal of Strain Analysis, Vol II, 1, 170-177 (1972).

3. Berghaus, D. G. and H. B. Peacock, Deformation and Strain Analysis for High Extrusion Ratios and Elevated Temperatures," Proceedings of the 1984 V International Congress on Experimental Mechanics, Montreal, Canada, June 10-15, 1984.

4. Madrano, R. E., P. P. Gillis, C. Hinesby, and H. Conrad, "Application of Visioplastic Techniques to Axisymmetric Extrusions," Metal Forming: Interrelation Between Theory and Practice: Proceedings of a Symposium on the Relation Between Theory and Practice in Metal Forming (Cleveland, Ohio, October 1970), p. 85-107, Plenum Press, New York (1971).

5. Lambert, E. R. and S. Kobayashi, "A Theory on the Mechanics in Extrusion Through Conical Dies," Part I of the Air Force Materials Laboratory Technical Report, AFML-TR-68-4, January 1968.

Table I - Extrusion Parameters for Aluminum Billet Extrusions

	Extrusion Ratio			
	1.9	7.4	12.4	12.4
Die Exit Diameter, cm. (in.)	6.5 (2.560)	3.3 (1.284)	2.5 (0.994)	2.5 (0.994)
Temperatures, °C				
Container	350	361	174	351
Die*	344	355	176	361
Billet	425	425	426	421

*Semicone Angle = 45°

Table II - Average Circumferential Strains at the Die Exit

Extrusion Ratio, R	Tooling Temp., $(\bar{T})$ °C	Experimental ε_θ	Logarithmic $\varepsilon_{\theta l}$*
1.9	354	0.280	0.295
7.4	354	1.00	1.00
12.4	175	1.29	1.29
12.4	354	1.24	1.26

*Calculated based on experimental outermost flowline

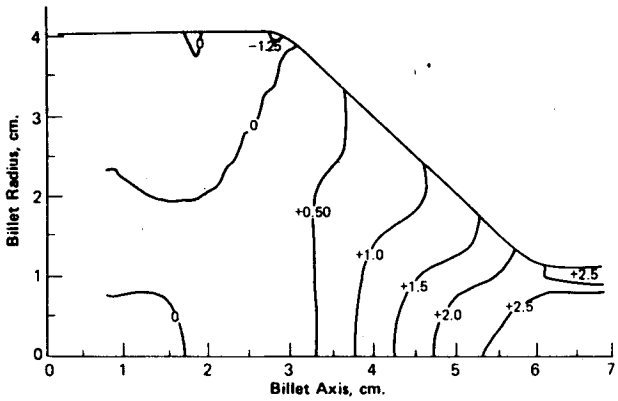

a) Low Tooling Temperature ($\bar{T}$ = 175°C)

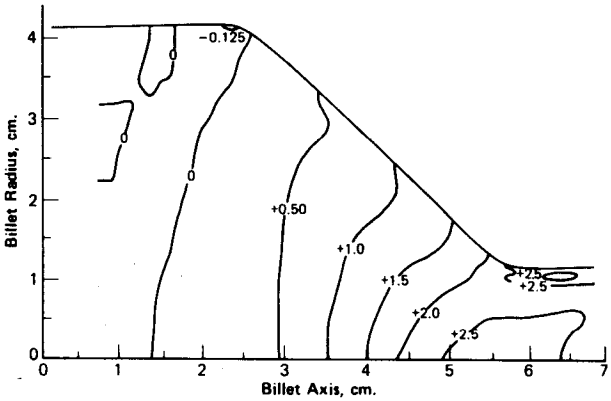

b) High Tooling Temperature ($\bar{T}$ = 354°C)

Fig. 1 - Strain Parallel to the Flowlines, ε_a, for Different Tooling Temperatures (R = 12.4)

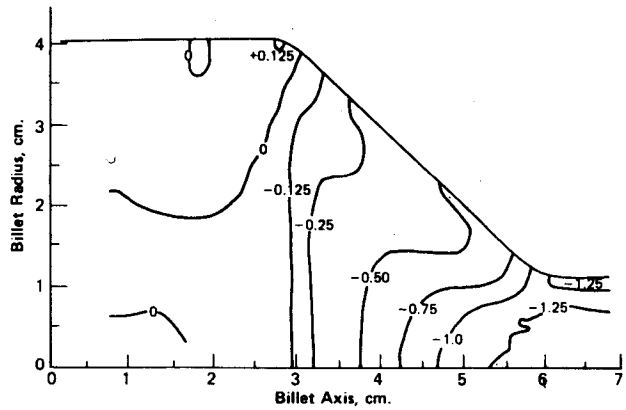

a) Low Tooling Temperature ($\bar{T}$ = 175°C)

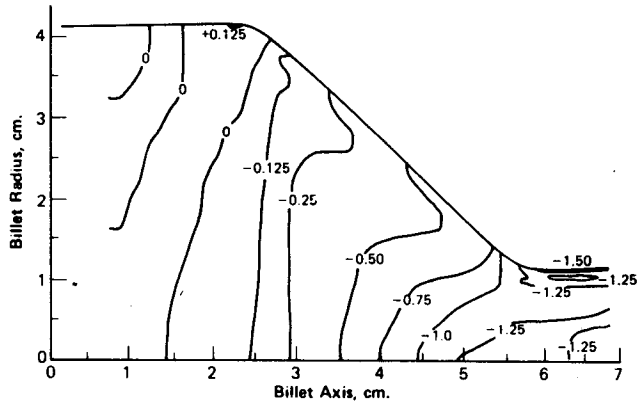

b) High Tooling Temperature ($\bar{T}$ = 354°C)

Fig. 2 - Strain Normal to the Flowlines, ε_b, for Different Tooling Temperatures (R = 12.4)

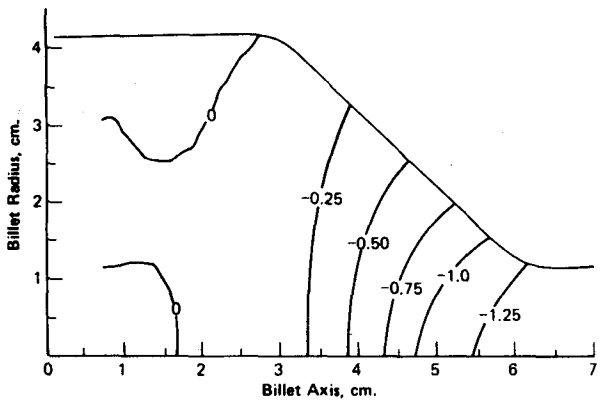

a) Low Tooling Temperature ($\bar{T}$ = 175°C)

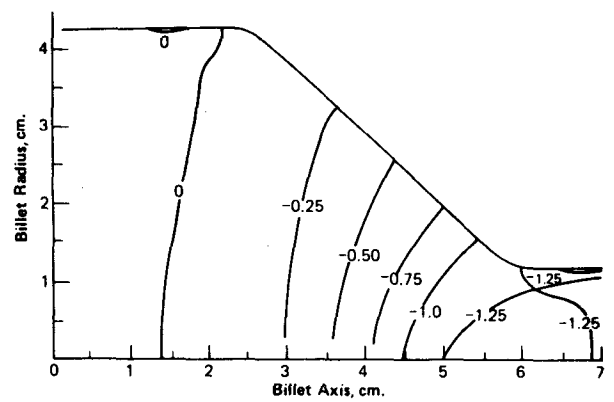

b) High Tooling Temperature ($\bar{T}$ = 354°C)

Fig. 3 - Circumferential Strain, ε_θ, for Different Tooling Temperatures (R = 12.4).

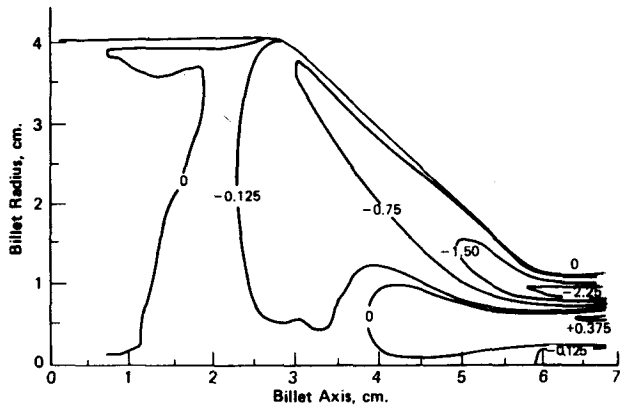

a) Low Tooling Temperature ($\bar{T}$ = 175°C)

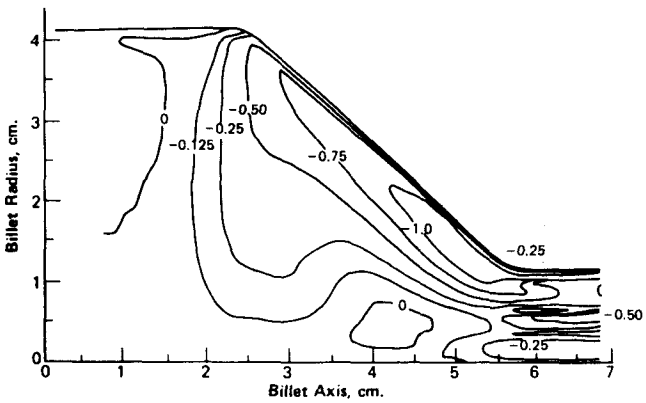

b) High Tooling Temperature ($\bar{T}$ = 354°C)

Fig. 4 - Accumulated Shear, ε_{ab}, for Different Tooling Temperatures (R = 12.4)

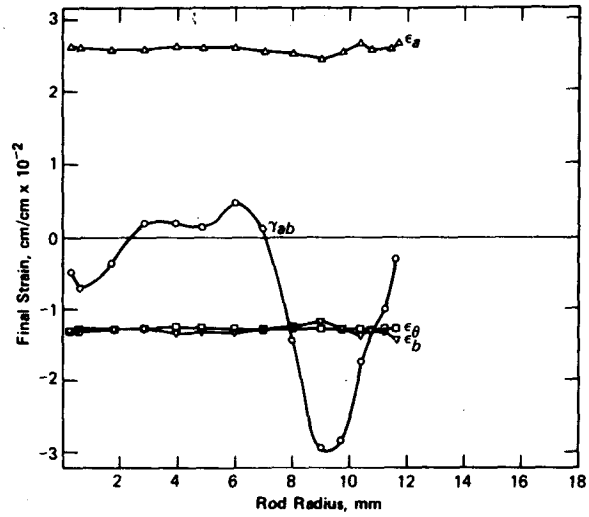

a) Low Tooling Temperature ($\bar{T}$ = 175°C)

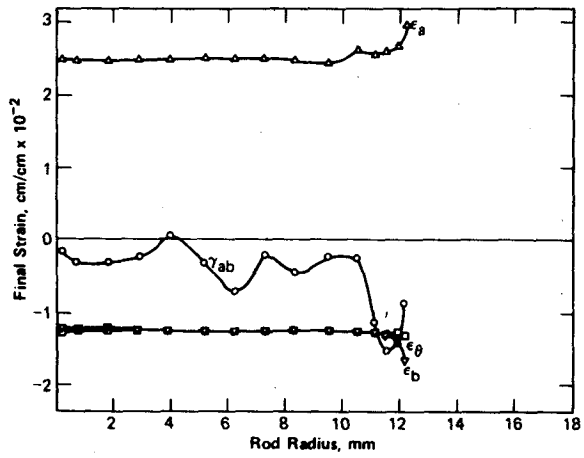

b) High Tooling Temperature ($\bar{T}$ = 354°C)

Fig. 5 - Final Extensional Strains and Accumulated Shear for Low and High Tooling Temperature (R = 12.4).

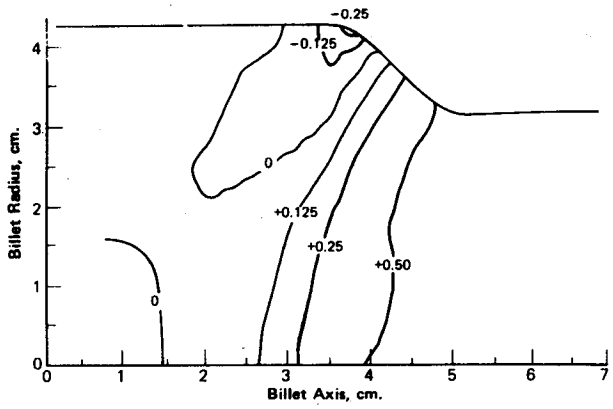

a) Extrusion Ratio of 1.9

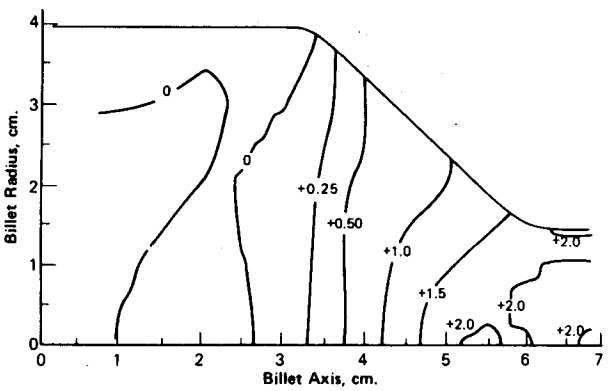

b) Extrusion Ration of 7.4

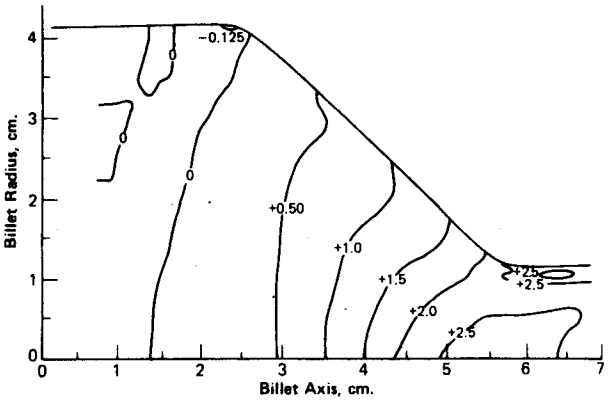

c) Extrusion Ratio of 12.4

Fig. 6 - Strain Parallel to Flowlines, ε_a, for Different Extrusion Ratios (T = 354°C).

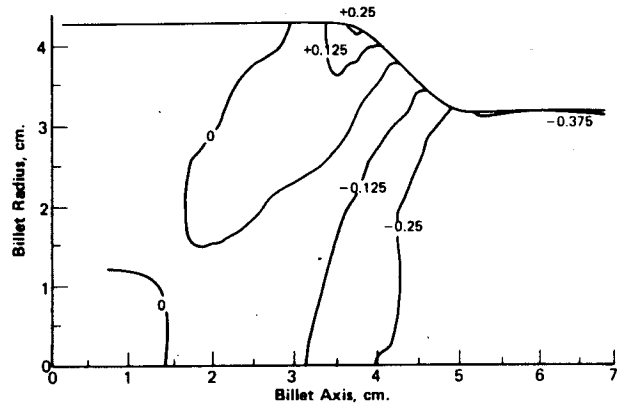

a) Extrusion Ratio of 1.9

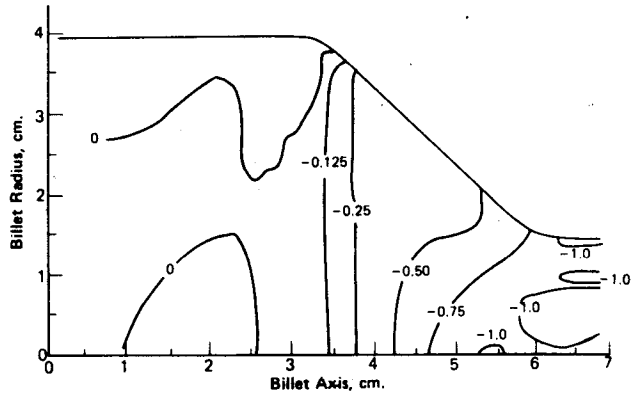

b) Extrusion Ration of 7.4

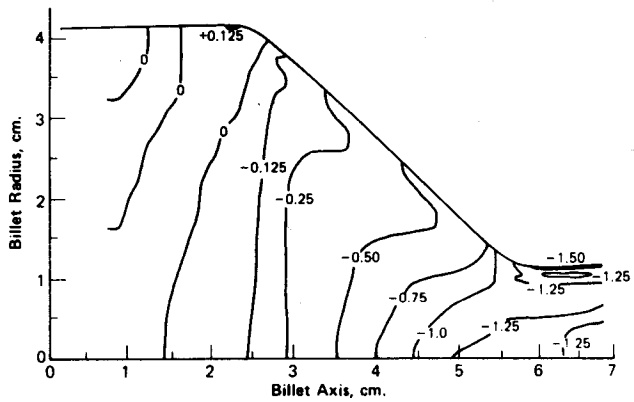

c) Extrusion Ratio of 12.4

Fig. 7 - Strain Normal to Flowlines, ε_b, for Different Extrusion Ratios (T = 354°C)